Eur. Phys. J. B **6**, 143–155 (1998)

THE EUROPEAN PHYSICAL JOURNAL B

Statistical analysis of the transition to turbulence in plane Couette flow

S. Bottin and H. Chaté

CEA — Service de Physique de l'État Condensé, Centre d'Études de Saclay, 91191 Gif-sur-Yvette, France

Received: 10 April 1998 / Revised: 22 June 1998 / Accepted: 24 June 1998

Abstract. We argue on general grounds that the transition to turbulence in plane Couette flow is best studied experimentally at a statistical level. We present such a statistical analysis of experimental data guided by a parallel investigation of a simple coupled map lattice model for spatiotemporal intermittency. We confirm that this generic type of spatiotemporal chaos is relevant in the context of plane Couette flow, where the linear stability of the laminar regime at all Reynolds numbers insures the necessary local subcriticality. Using large ensembles of similar experiments, we show the existence of a well-defined threshold Reynolds number above which a unique, turbulent, intermittent attractor coexists with the laminar flow. Furthermore, our data reveals that this transition to spatiotemporal intermittency is discontinuous, *i.e.* akin to a first-order phase transition.

PACS. 47.20.-k Hydrodynamic stability – 47.20.Ky Nonlinearity (including bifurcation theory) – 47.27.Cn Transition to turbulence – 05.45.+b Theory and models of chaotic systems

The plane Couette flow, in which a fluid layer is sheared between two parallel plates moving with opposite tangential velocities, offers one of the most intriguing frameworks for studying the transition to turbulence. Whereas the simple linear laminar velocity profile is stable at all Reynolds numbers R [1], it is well known that finite-amplitude perturbations may trigger abrupt, localized transitions to turbulent spots if R is sufficiently large [2–4].

Despite an already considerable literature on plane Couette flow, the statistical aspects of this important case of transition to turbulence have so far been largely unexplored. Most works were performed from a rather conventional fluid dynamics point of view, *e.g.* in order to uncover particular nonlinear solutions not continuously related to the laminar flow [5,6], or to extend the stability analysis of the laminar profile to account for long "transients," by exploiting the so-called non-normality of the linear operator [7].

At a more qualitative level, it has been recognized that plane Couette flow possesses all the necessary ingredients for exhibiting spatiotemporal intermittency, a generic type of spatiotemporal chaos akin to the behavior of directed percolation-like models above threshold [8]. Indeed, the sustained disordered regimes observed at relatively high Reynolds numbers, in which turbulent spots move, grow, decay, split, and merge, have been described in terms of a "contact process", *i.e.* a process in which active/turbulent regions may invade absorbing/laminar domains where disorder cannot spontaneously emerge [3]. Even though spatiotemporal intermittency refers to spatially-extended deterministic systems, this high-dimensional chaotic behavior is best described and analyzed from a statistical viewpoint, as suggested by the analogy sketched above with probabilistic cellular automata with one absorbing state, a class of models much studied in non-equilibrium statistical mechanics (see, *e.g.*, [9]). Furthermore, as argued in detail below, the spatiotemporal intermittency framework implies that the turbulent regimes of plane Couette flow *must* be approached statistically. As a matter of fact, this was implicitly realized by Daviaud *et al.* [3], who presented results based on small ensembles of about 10 experiments.

In this work, we present extensive experimental results on the transition to turbulence in plane Couette flow. Large ensembles of similar experiments were performed to provide meaningful statistics. Their analysis is guided and supplemented by parallel results obtained through numerical simulations of a coupled map lattice model showing spatiotemporal intermittency. Our general conclusion is that the experimental results are fully consistent with a discontinuous (first-order like) transition to spatiotemporal intermittency. This confirms the findings of a recent short paper [10], of which our work can be seen as an extension.

The paper is organized as follows. In Section 1, we briefly present the experimental setup and detail the proposed analogy between the turbulent regimes of plane Couette flow and spatiotemporal intermittency. The basic results for the transition to spatiotemporal intermittency are recalled in Section 2, with the help of the coupled map lattice model mentioned above to guide the statistical analysis of experimental results. A general definition

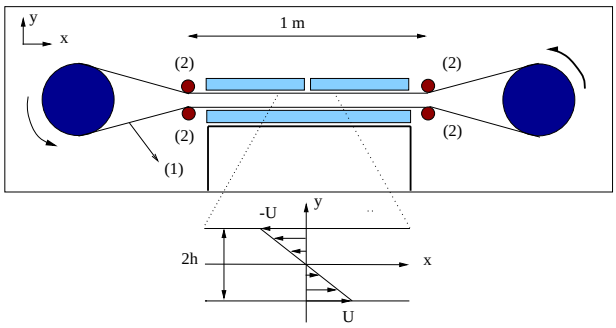

Fig. 1. Experimental setup with (1): transparent plastic belt, (2): guiding cylinders, immersed in a tank filled with water, and velocity profile of the basic flow).

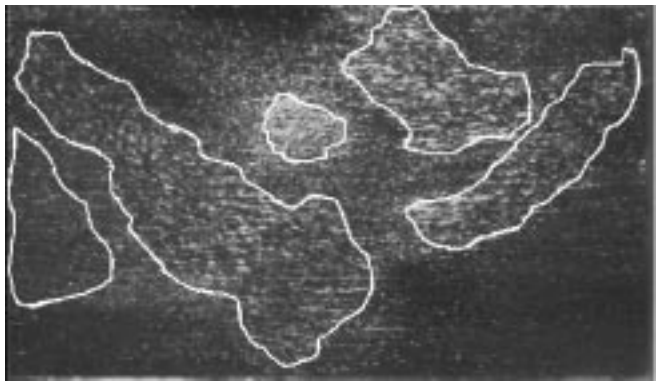

Fig. 2. Typical snapshot of the flow in a sustained spatiotemporal intermittency at $R = 320$. This image was taken during an experiment realized with a gap $2h$ two times smaller than that used in the statistical analysis presented here ($2h = 3.5\,\mathrm{mm}$).

of the threshold Reynolds number in plane Couette flow is given in Section 3. In Section 4, we revisit the "quench" experiments already presented in [10], in which a highly-turbulent system is suddenly brought to lower R values, and compare them to similar numerical experiments performed on our simple reference model. Section 5 is devoted to "bubble" experiments of the type first performed by Daviaud *et al.* [3], where a controlled, localized perturbation is introduced into the laminar flow. A detailed statistical analysis is presented both below and above threshold, together with the coresponding results obtained on the reference model. We conclude (Sect. 6) with a general discussion of our results and perspectives at both the experimental and modeling levels.

1 General setting

1.1 Experimental setup and basic flow regimes

The experimental setup has already been described in details elsewhere [3]. Here, we recall only its main characteristics. The flow is realized inside a long belt of transparent plastic (1) maintained in tension and guided by two rollers (2), as seen in Figure 1. We use a gap $L_y = 2h = 7\,\mathrm{mm}$ between the two "plates". The control parameter is the velocity $\pm U$ (measured in the lab frame) of the plates, so that the Reynolds number is $R = Uh/\nu$ with ν the kinematic viscosity of water, the fluid used. The spanwise and streamwise aspect ratios are, respectively, $\Gamma_z \equiv L_z/2h \simeq 35$ and $\Gamma_x \equiv L_x/2h \simeq 190$. The measurements reported in this work derive from image-processing of a video recording of the central plane between the plates. To this aim, the flow is seeded with iriodin, and illuminated by a thin laser sheet in the central (x, z) plane.

At large Reynolds number, a highly turbulent state arises spontaneously, the small inhomogeneities and/or boundary effects being large enough to destabilize the laminar flow. Decreasing R slowly, turbulence is only intermittent: a typical snapshot (Fig. 2) reveals strongly disordered patches separated by regions in which the flow is very close to the laminar profile. At any given point in space, the recorded activity is also intermittent, in the form of a "telegraphic" signal composed of a succession of turbulent and laminar periods. Such regimes, which do *not* arise when increasing R "adiabatically" (*e.g.* when increasing R by small steps separated by several minutes), can be sustained indefinitely in our experiment at large enough R. Decreasing R further, turbulent spots eventually disappear, and the fully laminar flow is always observed asymptotically.

The fine structure of the turbulent regions is still mostly unknown, and has motivated numerous hydrodynamical studies. From the view point adopted here, it is largely irrelevant, as long as the fronts separating the two basic states of the flow are sharp enough. The streamwise vortices often detected around the edges of turbulent regions [11] set the scale of the front width. This rather well-defined width is the condition for a reliable and meaningful detection by image processing.

1.2 Analogy with spatiotemporal intermittency

As argued above, the intermittent character of the flow both in space and time allows us to distinguish two different *local* states. The laminar state can be defined rather accurately by reference to the stable linear velocity profile. The "turbulent" state, however, largely reflects our (volontary) ignorance of the structure of turbulent spots. This reduction to two states should be seen as a first-order approximation which, nevertheless, should not influence the results presented below, at least at a qualitative level.

A crucial point is that the two local states are asymmetric: the linear stability of the basic flow implies that large laminar regions may only get destabilized at their boundaries with turbulent spots or under the influence of external finite-amplitude perturbations (in the assumed absence of long-range interactions). This is the case at least in an ideal (noiseless) experiment performed in an infinite (x, z) domain. In practice, there is always a Reynolds number above which residual noise or imperfections at the boundaries are strong enough to trigger turbulent regions, given that the metastability of the laminar state "decreases" with R [12,13].

Nonetheless, the essential ingredients of spatiotemporal intermittency are present: one can picture — at a crude but informative level — the complex space-time evolution of the intermittent regime as a *contact process* between two states, one of which (the laminar one) is *absorbing*. This vocabulary refers to a large class of statistical mechanics problems, of which directed percolation is the most famous [9]. However, this privileged situation can be somewhat misleading, since directed percolation is known mostly for exhibiting a continuous (second-order like) phase transition marking the limit of sustained existence of active sites. As a matter of fact, contact processes such as two-state probabilistic cellular automata with one absorbing state do not all exhibit continuous transitions. For space dimensions of two and higher — the case of interest here — discontinuous transitions are possible as well [14].

To illustrate these ideas, in the next section we do not use probabilitic cellular automata such as those evoked above, but, rather, introduce a simple spatially-extended dynamical system for which disorder arises from deterministic chaos. This is a choice motivated only by our will to stay within a framework sometimes thought more suitable for fluid flows.

2 A minimal model of reference

The analogy mentioned above between spatiotemporal intermittency and contact processes such as directed percolation, originally suggested in a seminal paper by Pomeau [15], was investigated using various kinds of spatially-extended dynamical systems [16]. In order to deal with the "core" issues and only them, a minimal model was designed in the form of a coupled map lattice, *i.e.* a discrete-time, discrete-space dynamical system [17]. In the following, we consider the two-dimensional version of this model, and revisit the results obtained in [18] in the context of the transition to turbulence in plane Couette flow.

Space is represented by a square lattice with real variables $X_{i,j}$ at each node updated synchronously at discrete timesteps according to:

$$X_{i,j}^{t+1} = (1-\varepsilon) f(X_{i,j}^t) + \frac{\varepsilon}{4}(X_{i+1,j}^t + X_{i-1,j}^t + X_{i,j+1}^t + X_{i,j-1}^t) \quad (1)$$

where ε is the diffusive coupling strength. The local map f is defined by (Fig. 3):

$$f(X) = \begin{cases} rX & \text{if } X \in [0, 1/2] \\ r(1-X) & \text{if } X \in [1/2, 1] \\ k(X - X^*) + X^* & \text{if } X > 1 \end{cases} \quad (2)$$

with $X^* = (r+2)/4$, $|k| < 1$, and $r > 2$ ($r = 3$ in this work).

Although by no means unique, this choice of f reflects the basic requirements for spatiotemporal intermittency: as long as $X < 1$, the evolution under f is chaotic (f is then just a tent map of slope $r > 1$). This chaos is transient only because the unit square is not invariant

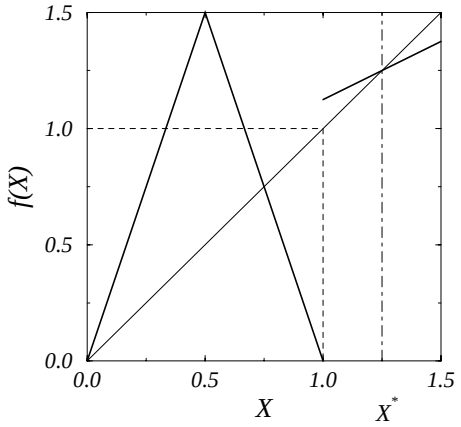

Fig. 3. Local map f of the coupled map lattice model.

($r > 2$), and one eventually reaches a fixed point when $X > 1$. The local phase space of f is thus a chaotic repellor connected to a stable fixed point. This provides a natural distinction between a "turbulent" ($X < 1$) and a "laminar" local state. When ε is small, the evolution of the lattice is similar to the uncoupled case: every site eventually reaches a fixed point whatever its initial value. For large ε, however, the influence of neighbors can be strong enough to bring a site back into the turbulent state, and spatiotemporal chaos can be sustained: the local chaotic repellor gives rise to a global chaotic attractor. Of course, the emergence of sustained spatiotemporal intermittency requires that at least some sites initially be in the turbulent state. In other words, the laminar state is absorbing: if a site and its neighbors are laminar at time t, then the central site remains laminar at time $t+1$ independent of the value of ε.

The chaotic regimes, intermittent in both space and time, are observed above some well-defined threshold value ε_c. At the crudest level, following the analogy with contact processes such as directed percolation, the transition can be monitored by the behavior of $\langle m \rangle$, the time-averaged turbulent fraction, or, equivalently, the mean concentration of active sites, treated here as the "order parameter".

It was shown numerically in [18] that the transition occuring at ε_c can indeed be considered as a phase transition similar to that of contact processes. It was further shown that its nature depends upon the parameter used: for $k = 1$, the transition is continuous (second-order like), *i.e.* the order parameter goes continuously to zero when decreasing ε, like $\langle m \rangle \sim (\varepsilon - \varepsilon_c)^{-\beta}$ with a critical exponent $\beta \simeq 0.52$ close to, but different from, the corresponding directed percolation value ($\beta_{DP} \simeq 0.58$) (Fig. 4a). For $k < 1$, however, the transition is discontinuous (first-order like) and $\langle m \rangle$ jumps to zero at $\varepsilon = \varepsilon_c$ (Fig. 4b).

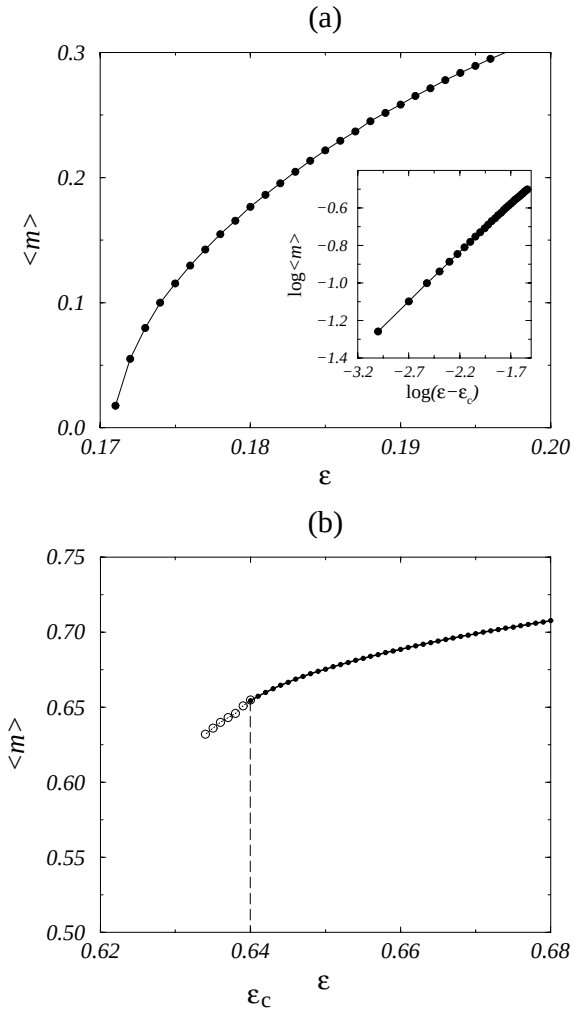

Fig. 4. Time-averaged turbulent fraction *vs.* coupling parameter in the coupled map model. (a) $k = 1$ (continuous transition) $\langle m \rangle$ goes continuously to zero at $\varepsilon_c \simeq 0.171$. Inset: log-log plot showing the algebraic decay of $\langle m \rangle$. (b) $k = 0.5$ (discontinuous transition) $\langle m \rangle$ jumps to zero at $\varepsilon_c \simeq 0.64$. The dashed line indicates the metastable states observed below threshold.

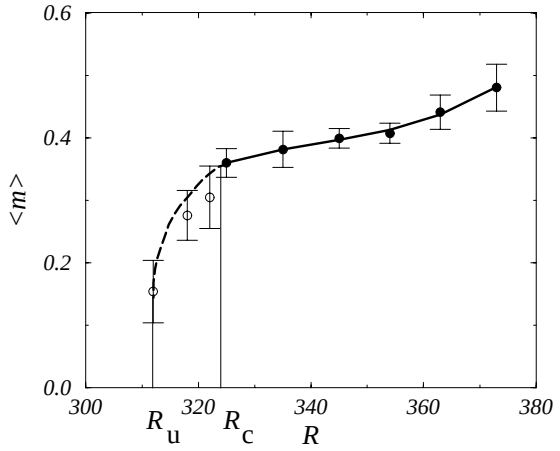

Fig. 5. Mean turbulent fraction *vs.* Reynolds number for plane Couette flow. Points linked by the thick solid line correspond to R values at which turbulence "never" dies out (t_{max} of the order of 600 s). The points linked by the dashed line were estimated from the metastable plateaus characterizing the weakly repelling nature of the intermittent phase below threshold (see Fig. 6a). The limit value R_u marks (very approximately) the limit of existence of these plateaus.

3 Defining a threshold in plane Couette flow

The brief description, given in Section 1.1, of the various regimes observed in plane Couette flow suggests the existence of a threshold Reynolds number R_c below which all turbulence eventually dies out, and above which sustained disordered regimes may be observed. It is also clear from the previous section that this definition coincides with that of ε_c in our minimal model for spatiotemporal intermittency. In terms of the total phase space of the system, no chaotic attractor exists below threshold. This is equivalent to saying that the laminar flow is the global attractor of the system below threshold only if there does not exist any stable solution other than the laminar flow.

Despite its simplicity, the above definition has only been investigated quantitatively recently [10]. One of its inherent problems is that it implicitly refers to the behavior of an infinite system observed over infinitely long periods. In practice, one always has to deal with finite-size systems and finite observation times, although such size effects can usually be accounted for, and rather safe extrapolations to the infinite-size limit can be made. In our experimental system, for example, one can measure $m(t)$ (defined here as the total surface occupied by turbulent regions over $L_x \times L_z$) and choose a maximal duration t_{max} past which turbulence is declared to be "sustained". This procedure yields an effective threshold $R_c(t_{max})$, which should converge to some limit value, as $t_{max} \to \infty$. Finite-size effects could also be estimated in the same way, ultimately leading to the actual threshold value.

Unfortunately, this approach is too tedious to be followed completely. One can, however, at a fixed system size, choose a single large value of t_{max} (say, $t_{max} = 600\,\mathrm{s}$), and record $\langle m \rangle$ for the R values for which disorder was sustained up to t_{max}. Figure 5 shows the results for our experiments. Remarkably, the recorded values of $\langle m \rangle$ decrease only slightly with R and suddenly jump to zero at some effective threshold around $R_c \simeq 323 \pm 2$. This indicates that the transition is discontinuous, a fact confirmed by our other experiments.

There exist better ways to estimate the threshold and to determine the nature of the transition. They have been explored in detail for simple models of spatiotemporal intermittency (see, *e.g.* [17,18]). At the experimental level, one is more constrained, but meaningful protocols can be followed. As explained below, they are intrinsically *statistical* and involve determining probabilities, expectation values, *etc.*, from an *ensemble of similar experiments.* We now present these results and discuss them in detail

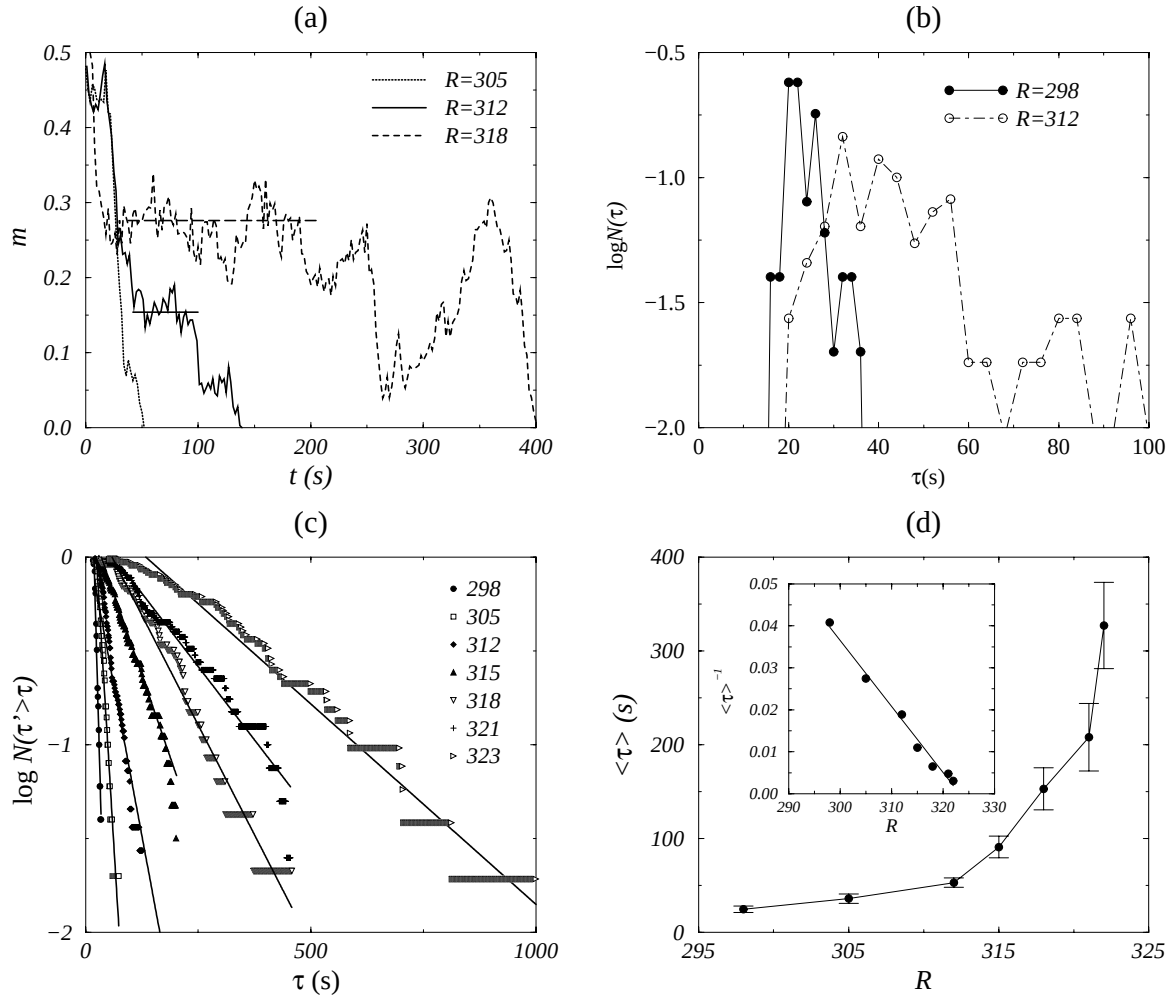

Fig. 6. Quench experiments in plane Couette flow. (a) Typical time series of m obtained at $R = 305$, 312 and 318. The horizontal lines represent the estimated values of $\langle m \rangle$ on the metastable plateaus. One might be tempted to distinguish other, lower "plateaus" from these time series; they might be considered as an indication of the "separatrix" between the laminar attractor and the intermittent repellor. Note that $R = 305$ is a Reynolds number lower than R_u. (b) Logarithms of histograms of lifetimes after quench (ensembles of 50-100 experiments). (c) Logarithms of cumulated histograms of lifetimes after quench. (d) $\langle \tau \rangle$ *vs.* R; inset: $1/\langle \tau \rangle$ *vs.* R.

with the help of similar statistics gathered from numerical simulations of our minimal reference model.

4 Quench experiments

One efficient way of controlling time-effects in our problem is to perform quench experiments: the system is first brought to a steady regime far above threshold where initially introduced turbulence occupies most of space, and for which decay is never observed [19]; the control parameter is then decreased suddenly. If the control parameter value to which the system was quenched is below threshold, then disorder dies out in a finite time τ. The threshold R_c or ε_c is defined as the value above which $\langle \tau \rangle$, the ensemble average of τ over a large set of experiments, is infinite [20]. This procedure has the advantage of being based only on finite-time quantities, but is not free from finite-size effects. For a given system size, it yields an effective threshold *a priori* above the asymptotic (infinite-size) value.

4.1 Experimental results

Series of quench experiments on our plane Couette flow system were performed by suddenly decreasing the Reynolds number from a steady, highly-turbulent regime observed at $R = 380$. For low R values, the time series of m was recorded and τ was detected (Fig. 6a). About 50–100 experiments were done for each R value, and the distribution of τ values was constructed. The direct histograms of τ (Fig. 6b) reveal that the mean, the most probable value, and the smallest value recorded all increase when R increases. The cumulated histograms (Fig. 6c) allow a better determination of the exponential tail at large τ. The mean lifetime $\langle \tau \rangle$ can then be measured from the slope of this tail in a lin-log plot, or simply from the mean of the distribution. These two values are close to one other,

and behave in the same manner as a function of R. In particular, $\langle\tau\rangle$ increases continuously and strongly with R, suggesting a divergence at some finite R value. Of the different simple possible fits for this data, the most satisfactory yields $\langle\tau\rangle \sim 1/(R_c - R)$ with $R_c \simeq 323 \pm 2$ (Fig. 6d).

4.2 Numerical results

Quench experiments on the simple coupled map lattice defined in Section 2 have been performed for $k = 1$ (continuous transition) and $k = 0.5$ (discontinuous transition). In both cases, the distributions of τ values exhibit exponential tails (Figs. 7a, 8a). In both cases, the mean and the most probable value increase when approaching threshold. The mean lifetime of turbulence $\langle\tau\rangle$ can be defined either from the tails or simply from the mean of the distribution. In the continuous case, however, a region of algebraic distribution appears in the critical region near ε_c. In both cases, a divergence of $\langle\tau\rangle$ is observed when increasing ε toward ε_c. Thus the qualitative behavior of $\langle\tau\rangle$ is similar to that observed in the laboratory experiments, but without distinguishing between continuous and discontinuous transitions.

At a quantitative level, the divergence of $\langle\tau\rangle$ differs. In the case of a continuous transition, one expects $\langle\tau\rangle \sim (\varepsilon_c - \varepsilon)^{\nu_\parallel}$ with a non-trivial critical exponent $\nu_\parallel$. The calculations presented in Figure 7b lead to $\nu_\parallel \simeq 1.18$. For the discontinuous case studied, ($k = 0.5$), we find a simple integer exponent (Fig. 8b): $\langle\tau\rangle \sim 1/(\varepsilon_c - \varepsilon)^2$.

The two cases also differ when one considers the time series of the mean turbulent fraction $\langle m\rangle(t)$ (Figs. 7c, 8c). Near threshold, an algebraic decay of $\langle m\rangle(t)$ is observed for $k = 1$, whereas the discontinuous case presents a typical plateau —the signature of the metastability of the intermittent phase near and below threshold— followed by a sudden decay to zero. In this last case, one also observes large variations from run to run, as the duration of the metastable transient changes.

4.3 Discussion

The experimental data sets are still too limited to allow a precise estimate of the exponent governing the divergence of $\langle\tau\rangle$. Nevertheless, the best fit $\langle\tau\rangle \sim 1/(R_c - R)$ suggests a simple value of the exponent, consistent with the discontinuous case. The behavior of $\langle m\rangle(t)$ cannot be resolved by our experiments either. However, the inspection of individual experiments shows that, near and below threshold, $m(t)$ often lingers for long periods of time around some well-defined value before eventually experiencing a fatal fluctuation, after which turbulence dies out (Fig. 6a). These individual events indicate the metastable character of the intermittent phase below threshold. They are also observed near and below threshold of the *discontinuous* transition in our simple model, but not in the continuous case. They are in fact at the origin of the plateau of Figure 8c for $\varepsilon = 0.63$.

In terms of global phase space structure, our data indicates that the intermittent chaotic attractor present above threshold becomes a (weakly) repelling set below threshold, in agreement with the picture of a first-order-like transition (the active phase becomes metastable below the "Maxwell" point) [15]. This allows the extension of the $\langle m\rangle(R)$ curve beyond R_c (Fig. 5), using the values of the metastable plateaus.

All of these elements lead to a conclusion as to the discontinuous character of the transition to turbulence in plane Couette flow. The thresholds determined by quench experiments are, *a priori*, slightly overestimated because they are not free from finite-size effects [21]. We now turn to experiments which can be considered free from size effects, where localized perturbations are introduced into the laminar flow.

5 Bubble experiments

The general idea of the possible conditional stability of the laminar flow at high Reynolds numbers, led previous investigators to look for a way of creating controlled perturbations of tunable amplitude. Indeed, one could then hope to provide evidence for the existence of a "critical" amplitude above which perturbations would lead to sustained turbulence, and below which they would decay. Here, we perturb the laminar flow by the method used in [3,4,22]. In these experiments, a small jet is sent across the (x, z) plane due to small holes drilled in the middle of the belt, thus creating a small disordered "bubble". The duration and the amount of water injected are controlled. We now present new results using the same method, analyzing them within the general framework of spatiotemporal intermittency.

5.1 General considerations

First, we would like to stress that the above idea, which exploits the *local* subcriticality of the system, does not imply the *global* subcriticality (or discontinuous character) of the transition [16]. In the context of spatiotemporal intermittency, the existence of two distinct local states at "finite distance" from each other —the local subcriticality — is required, but the transition can be either supercritical/continuous or subcritical/discontinuous. However, as we discuss in detail below, this approach may indeed allow one to distinguish between the two possibilities.

Introducing localized perturbations may be *a priori* thought to be a good manner of avoiding finite-size effects. But other problems may arise which, briefly speaking, are related to the "efficiency" and the "relevance" of the mode of perturbation adopted.

Let us again take the point of view of the global phase space of the system, following Dauchot and Manneville [13]. In the laminar regime, the attractor is a stable fixed point. External arbitrary perturbations take the system

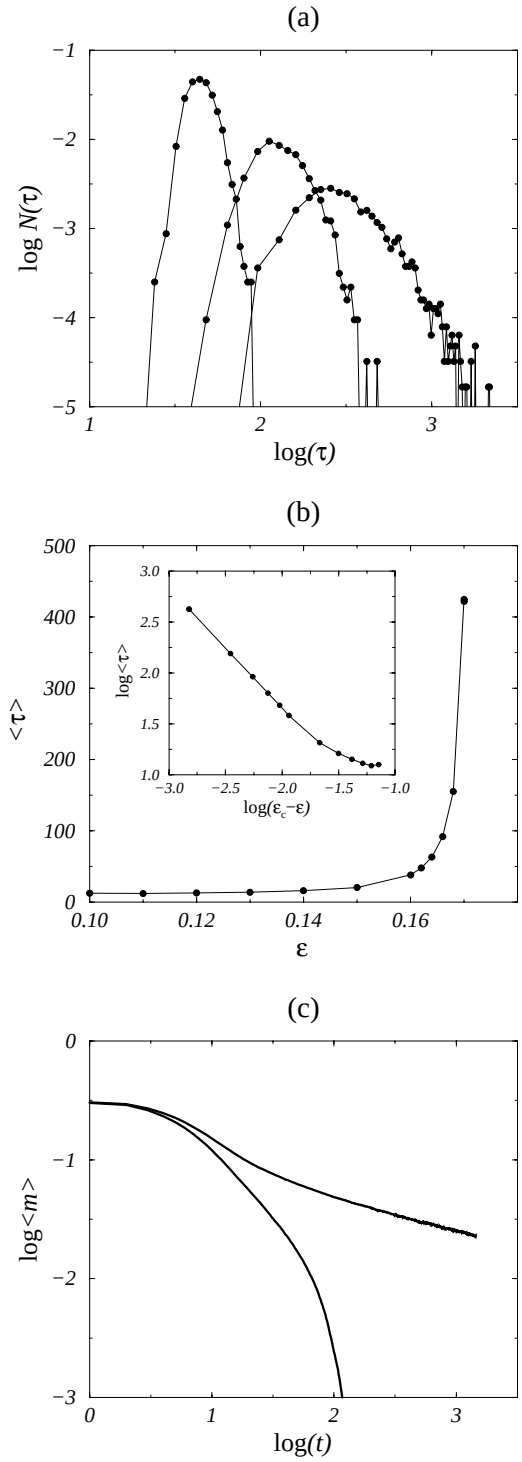

Fig. 7. Quench experiments in the simple reference model with $k = 1$. A lattice of 64^2 sites with periodic boundary conditions was thermalized at $\varepsilon = 0.2$ during 400 timesteps before the quench. Ensembles of 2000 runs. (a) Log-log plot of histograms of lifetimes after quench. From left to right: $\varepsilon = 0.162$, $\varepsilon = 0.168$, $\varepsilon = 0.170$. (b): $\langle\tau\rangle$ *vs.* R; insert: $\log\langle\tau\rangle$ *vs.* $\log(\varepsilon_c - \varepsilon)$ with $\varepsilon_c = 0.1715$. (c): $\log\langle m\rangle$ *vs.* $\log t$ near and below threshold ($\varepsilon = 0.171$, top, and $\varepsilon = 0.166$, bottom).

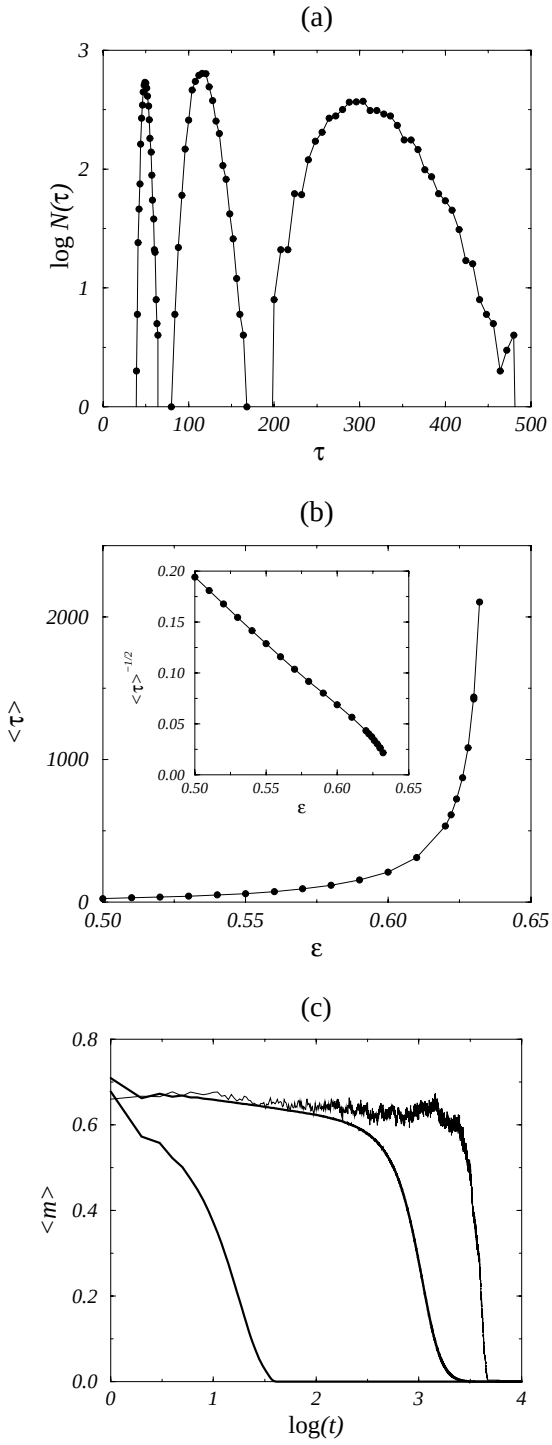

Fig. 8. Quench experiments in the simple reference model with $k = 0.5$. A lattice of 64^2 sites with periodic boundary conditions was thermalized at $\varepsilon = 0.72$ during 400 timesteps before the quench. Ensembles of 5000 runs. (a) Logarithms of histograms of lifetimes after quench. From left to right: $\varepsilon = 0.54$, $\varepsilon = 0.58$, $\varepsilon = 0.61$, (b): $\langle\tau\rangle$ *vs.* R; insert: $\langle\tau\rangle^{-1/2}$ *vs.* R. (c): $\langle m\rangle$ *vs.* $\log t$ (thick lines) near and below threshold ($\varepsilon = 0.63$, right, and $\varepsilon = 0.52$, left). The thin line shows the behavior of one single run at $\varepsilon = 0.63$, chosen for the long duration of the metastable transient.

to points of phase space either inside or outside the basin of attraction of the laminar attractor. A complete knowledge of the effect of the perturbation in phase space is a very hard problem, and one can only hope that the perturbation method does allow to leave the basin of attraction of the laminar solution. This *efficiency* of the method of perturbation used below and in earlier works [3,22] has fortunately been confirmed by experiments: strong enough jets at large enough Reynolds numbers do lead to sustained turbulence.

A further but related point concerns the *relevance* of perturbations, *i.e.* their ability to produce significantly different effective initial conditions. Given their arbitrary character, the perturbations can be considered to almost certainly bring the system out of its inertial manifold, *i.e.* the (finite-dimensional) subset of phase space to which all trajectories are attracted exponentially fast [23]. This manifold is not the attractor, but contains it; rather, it is the subset of phase space on which all transients evolve after a very short time. Varying the "amplitude" of the localized perturbations only makes sense if the "landing points" on the inertial manifold after the short transient are different.

Another problem inherent to introducing external perturbations is that *only* statistical arguments can then be used, a fact overlooked in previous studies. As always in an experimental context, the initial perturbation is not perfectly controlled. In addition, the transients following perturbations can be considered chaotic, and thus subject to sensitivity to initial conditions. Moreover, above threshold, the separatrix between the basins of attraction of the laminar flow and the chaotic/turbulent attractor is generically a very complex, fractal hypersurface in phase space. This implies that one *cannot* rely on single experiments to decide whether perturbations of a given amplitude lead to the turbulent attractor or not. Indeed, in the transitional region, the *same* experiments may lead to the decay of the initial bubble or to its expansion toward the turbulent attractor [24]. The only meaningful quantity is the *probability* p, over a large ensemble of experiments, to reach the turbulent regime. A threshold can then be defined as the point where this probability is, *e.g.*, $p = 1/2$. We note here that, while such considerations have been largely ignored in past studies of plane Couette flow, Darbyshire and Mullin adopted a similar point of view in their experiments on pipe flow [26].

We note finally that, in practice, experiments introducing localized perturbations are not free from time effects: the probability p can only be determined once a threshold t_{max} is chosen to discriminate between finite lifetimes ($\tau < t_{max}$) and "infinite" ones ($\tau > t_{max}$). Again, the thresholds thus defined are expected to converge to well-defined values as $t_{max} \to \infty$, but it is nearly impossible to study this convergence experimentally.

5.2 Experimental results

Series of experiments were performed by locally perturbing the laminar flow, either at a fixed Reynolds number and varying the amplitude of perturbation, or the opposite. Here, the amplitude A of the perturbation is just the velocity of the jet, its duration being kept fixed and very short (of the order of 10^{-1} s) compared to the viscous time scale (of the order of 1 s) [27].

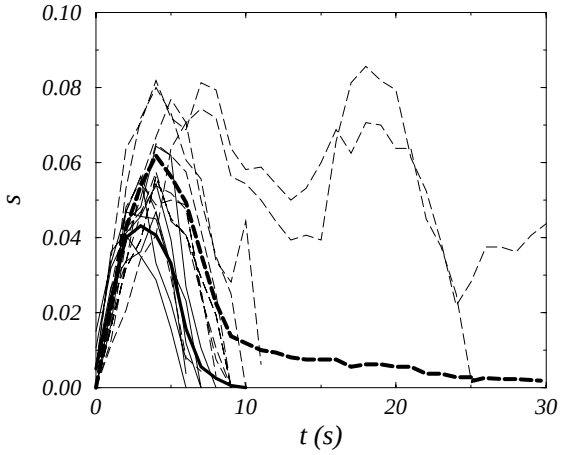

Fig. 9. Bubble experiments in plane Couette flow. Typical time series of s (thin lines) and time series of $\langle s \rangle(t)$ (thick lines) at $R = 330$ for $A = 1.6$ (solid lines) and $A = 3.1$ (dashed lines). For $A = 1.6$, all bubbles die in finite time ($p = 0$), while for $A = 3.1$ one-fourth of the initial bubbles grows to reach the intermittent attractor ($p \simeq 0.25$).

We recorded the time series of the area of the turbulent bubble normalized by the total size of the (x, z) plane. In order to stress that this quantity is not intensive, contrary to the turbulent fraction m of the quench experiments of Section 4, we denote it s. Figure 9 shows typical time series of s as well as $\langle s \rangle$. At given R and A values, the initial perturbation first grows quickly to a bubble of size s^* in a short time t^*, then either grows to reach the chaotic attractor or decays to zero, to die at time τ (Fig. 9). Quantities s^* and t^* are only well-defined statistically. We interpret the short transient time t^* leading to a well-defined turbulent "bubble" of size s^*, as the time needed to come back to the inertial manifold. This is corroborated by the fact that t^* hardly varies with A (Fig. 9), in accordance with an expected logarithmic dependence (the trajectory goes exponentially rapidly to the inertial manifold). On the other hand, s^* increases significantly with A (Fig. 9), which we take to be an indication of the relevance of the method of perturbation (different perturbations produce different effective initial conditions).

5.2.1 Above threshold: critical amplitude curve

We determined the location of the $p = 1/2$ curve in the (R, A) parameter plane. For each point studied, up to 100 experiments were performed, with a chosen cutoff $t_{max} = 300$ s. We checked that this value was large enough so that it has only limited influence on the thresholds. In fact, varying either A or R, p varies continuously

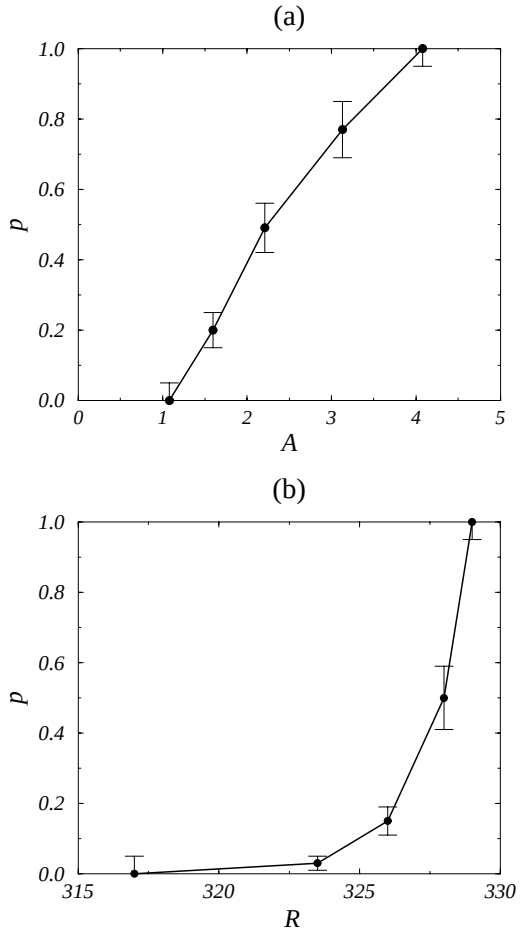

Fig. 10. Bubble experiments in plane Couette flow. Series of 50-100 experiments for each point (R, A). (a) probability p of reaching the turbulent attractor as a function of A for fixed $R = 335$. (b) same but at fixed amplitude $A = 4.75$ varying R.

but rather sharply from 0 to 1 (Fig. 10), allowing a precise determination of the threshold.

The final outcome of this long process is presented in Figure 11 and takes the form of a "critical amplitude" curve $A_c(R)$ in agreement with that presented by Dauchot *et al.* [22]. (We note that the critical amplitude curve of [22] can only be taken as indicative since it does not rely on statistical analysis.) Our results clearly show that stronger and stronger perturbations are needed to reach the turbulent state when R is decreased. The curve suggests a divergence of A_c at some finite value of R, as in ordinary first-order phase transitions. Given the limited range of variation of A_c available, it is impossible to determine the exact nature of this divergence. The data is however well-accounted for by a functional variation of the form: $A_c \sim (R - R_c)^\alpha$ with $R_c \simeq 325$ and $\alpha \simeq 0.7$. The validity of this fit is strengthened by the fact that the estimated threshold is equal, up to the experimental accuracy, to the value measured from quench experiments. We discuss the meaning of a divergence and this exponent below (Sect. 5.4).

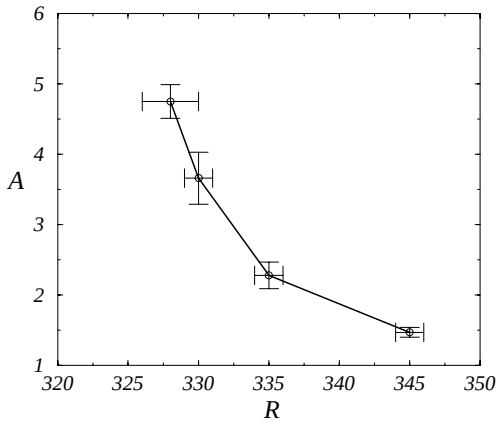

Fig. 11. Critical amplitude curve $A_c(R)$, as determined by the location of the $p = 0.5$ curve in the (A, R) plane.

5.2.2 Below threshold

Similar series of experiments were also performed at lower R values, and for perturbations amplitudes A such that the initial turbulent bubble *always* decay ($p = 0$ region).

The distributions of τ values thus obtained show a well-defined most probable value and a quickly decaying tail, which insures the existence of $\langle\tau\rangle$ (Fig. 12a). Note that, contrary to the quench histograms, here the most probable value does not increase significantly with R. The cumulated histograms (Fig. 12b) are also qualitatively different from those of quench experiments (compare to Figure 6c). Approaching threshold, say at fixed A and increasing R, $\langle\tau\rangle$ increases but does *not* diverge (Fig. 12c) as for the quench experiments (compare to Fig. 6d). All these findings are discussed in Section 5.4 below, in the light of the results obtained using our reference minimal model.

5.3 Numerical results

What should be, for our simple coupled map lattice model, the closest equivalent of the bubble experiments reported above is not clear *a priori*. However, the interpretation of the short transient time t^* and the corresponding bubble size s^* suggests that, within our simple model, the initial conditions for the equivalent experiments consist in creating a bubble of turbulent sites ($X < 1$) in an otherwise fully laminar ($X \geq 1$) medium. Here, the initial surface of the bubble, s_0, is taken as A, the "amplitude" of the perturbation. In the model, the initial perturbation thus created first quickly relaxes to a (usually smaller) bubble, as the system evolves back to its inertial manifold.

5.3.1 Around a continuous transition

In the case where our coupled map lattice model shows a continuous transition to spatiotemporal intermittency

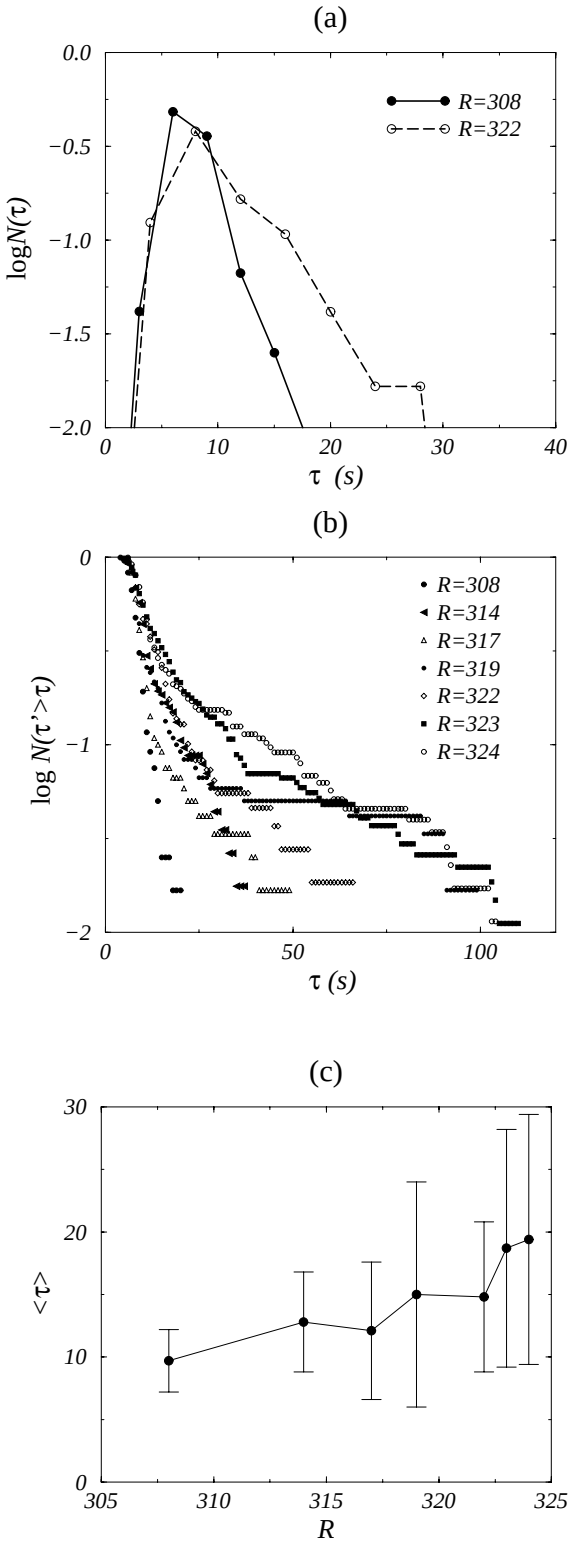

Fig. 12. Below-threshold bubble experiments in plane Couette flow. Series of 100-300 experiments. (a) Histograms of lifetimes for $R = 308$ and $R = 322$. (b) Cumulated histograms of lifetimes. A cut-off time of 120s was used to suppress "spurious" events (see text). (c) Variation of $\langle\tau\rangle$ with R for $A = 4.8$.

($k = 1$), bubble experiments statistics are clearly different from those of Section 5.2.

Approaching the threshold ε_c from below, the distribution of bubble lifetimes τ crosses over from exponential to algebraic tails, and the mean lifetime diverges like $\langle\tau\rangle = \kappa(s_0)(\varepsilon_c - \varepsilon)^{\nu_\parallel}$ where κ depends only weakly on s_0. Note that this dependence is the same as the one expected for quench experiments (see Sect. 4.2). This is one characteristic property of the continuous-transition case: all initial conditions with some active sites lead to the same asymptotic state.

Above threshold, the probability p, which in the directed percolation framework would correspond to the probability of percolating to infinity, behaves like $p = \kappa'(s_0)(\varepsilon - \varepsilon_c)^{-\beta}$. This implies that there is practically no dependence of the threshold on s_0, especially if a small p value is chosen to define the effective threshold.

The above behavior seems incompatible with the experimental results of Section 5.2. We will show that, on the contrary, there is good agreement in the case of a discontinuous transition to spatiotemporal intermittency in the model.

5.3.2 Around a discontinuous transition

We now report on bubble experiments in the case $k = 1/2$ where the transition is discontinuous. In fact, similar experiments were reported in [18], and used to demonstrate the existence, near and above threshold, of a critical size s_c which increases and seems to diverge when $\varepsilon \to \varepsilon_c$. Here, we present more extensive numerical simulations, showing results which shadow those obtained in plane Couette flow. Figure 13 shows the variation, along lines in the (ε, s_0) plane, of the probability p for reaching the intermittent attractor. Thanks to the simplicity of the model, ensembles of the order of 10^4 experiments with a cut-off time $t_{max} = 10^4$ are easily achieved, yielding very reliable statistics almost free from finite-time effects.

Such series of experiments were performed at various points in the (ε, s_0) plane. This allowed the determination of a $s_c(\varepsilon)$ curve (Fig. 14). As for the laboratory experiments, the value $p = 0.5$ was chosen to determine this curve. Again, we can try to fit a divergence of the form $s_c \sim (\varepsilon - \varepsilon_c)^\alpha$. The data does not allow us to conclude in any precise way, but ($\alpha = 1$, $\varepsilon_c = 0.67$) and ($\alpha = 2$, $\varepsilon_c = 0.66$) are two equally-plausible sets of simple values.

Below-threshold bubble experiments also yielded results very similar to those obtained by introducing localized perturbations in plane Couette flow. In particular, the mean lifetime $\langle\tau\rangle$ does not diverge at threshold (Fig. 15c). In the histograms of lifetimes (Fig. 15a), the most probable value does not increase when approaching threshold, as in the laboratory experiments (see Fig. 12a). We note, however, that the shape of the distributions have no *a priori* reason to be similar to those recorded in the laboratory, since the deterministic processes involved in the shrinking of a bubble in plane Couette flow are not accounted for by the model. Such a discrepancy is indeed suggested by the shape of the cumulated histograms in Figure 12b.

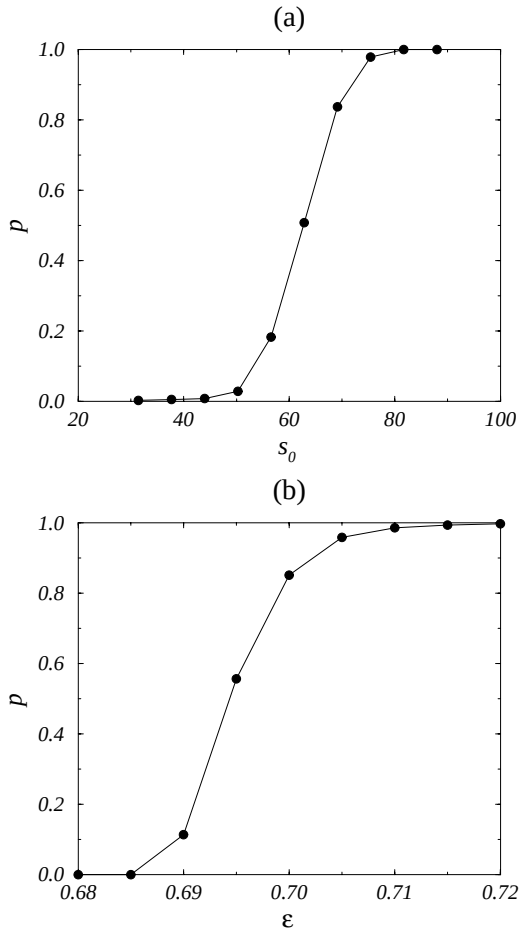

Fig. 13. Bubble experiments in the reference coupled map model with $k = 0.5$. (a) probability p of reaching the turbulent attractor as a function of s_0 for fixed $\varepsilon = 0.680$. Ensembles of 2000 runs, $t_{max} = 10000$. (b) same but at fixed amplitude $s_0 = 25$ varying ε.

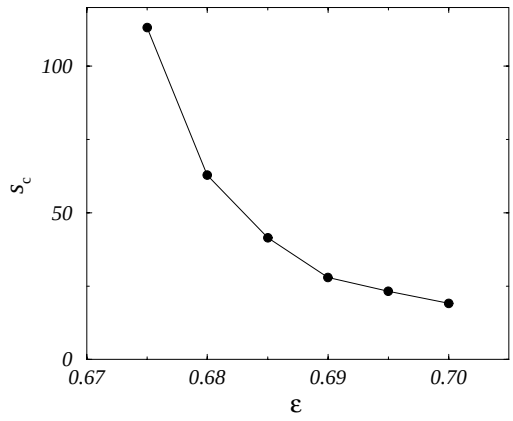

Fig. 14. Minimal model for $k = 0.5$: critical amplitude curve $s_c(\varepsilon)$, as determined by the location of the $p = 0.5$ curve in the (s_0, ε) plane.

5.4 Discussion

As already mentioned above, our experimental data from bubble experiments in plane Couette flow seem to be compatible only with the scenario of a discontinuous transition to spatiotemporal intermittency.

Nevertheless, the results obtained below but very near threshold call for further discussion. For R close to R_c, say $R = 324$, some experiments last exceptionally long, yielding τ values not "expected" from the main shape of the histograms. Our experimental setup does not allow us to explore the R-domain very near threshold with enough accuracy to accumulate precise enough statistics. Thus we cannot rule out a sudden divergence of $\langle\tau\rangle$ in a very small R-interval. But, in our opinion, the likely explanation for these rare events is the effectively-small size of our system (in particular, the boundaries might have a long "penetration length"), combined with some fluctuations in the Reynolds number (R is kept constant to an accuracy of $\delta R = 1$, see [10] for details). As a matter of fact, during these events, the initial bubble usually touches the boundaries, and its fate is then indistinguishable from the case of quench experiments. The recorded lifetimes are indeed of the order of those shown in Section 4.1. We believe these rare events should become rarer as the system size is increased. At any rate, their weight in the calculation of $\langle\tau\rangle$ remains so small that the qualitative picture is not changed.

Another point worth discussing is the status of very large initial bubbles. Indeed, if the created bubbles are large, they actually decay quickly in their bulk to a region of intermittent phase (*i.e.* usually with disconnected, smaller, turbulent patches), and the problem is not quite that of the fate of a localized perturbation: in the bulk, the situation is that of a quench experiment. This regime is not attainable in our experiment, due to its small effective size, but it can be observed in our simple model. This shows the difference between discontinuous transitions to spatiotemporal intermittency and ordinary first-order phase transitions, where the critical size — or, rather, the critical radius of curvature — diverges at threshold. In the intermittent case, laminar/absorbing domains are present, contrary to ordinary first-order transitions. Thus arguments such as those involving the local radius of curvature of the border of a (fully) active domain do not apply. They apply only to small bubbles, of sizes smaller than those observed spontaneously in the intermittent phase.

The series of bubble experiments performed above threshold have enabled us to explore a fairly limited portion of a critical amplitude curve. For the reference coupled map lattice model, the difficulty of reaching the immediate vicinity of the threshold is mostly due to the accompanying increase of τ (notwithstanding problems related to the status of large initial bubbles). In plane Couette flow experiments, there exist other factors preventing the study of large critical amplitude regimes. The method of perturbation is, in practice, limited to a certain range of amplitudes. But there may be deeper reasons: the choice

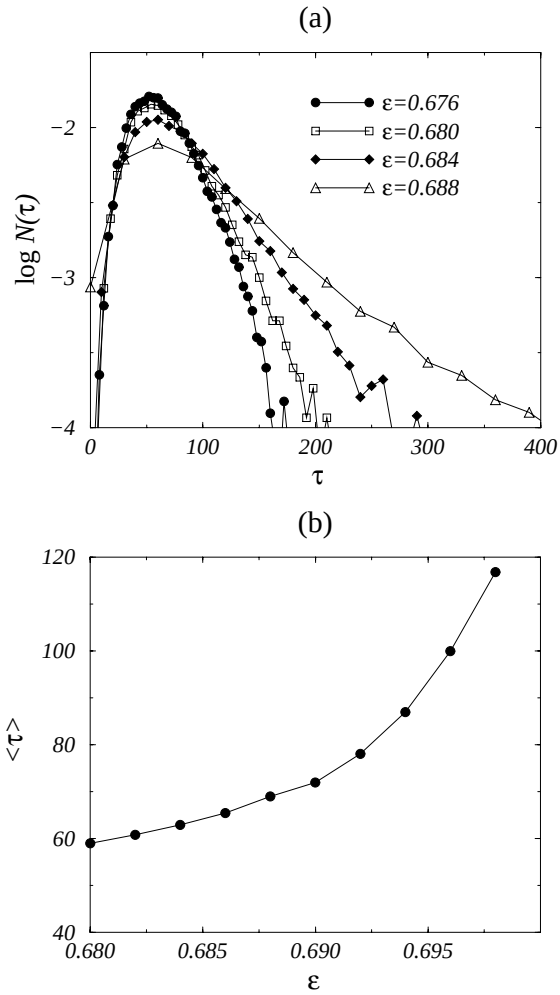

Fig. 15. Below-threshold bubble experiments in the coupled map lattice model for $k = 0.5$. Ensembles of 10000 runs, $t_{max} = 2000$. (a) Histograms of lifetimes for $s_0 = 25$ and $\varepsilon = 0.676$, 0.680, 0.684, 0.688. (b) Variation of $\langle\tau\rangle$ with ε for $s_0 = 25$. Note that the ε values shown here for convenience are larger than $\varepsilon_c \simeq 0.64$, but, of course, smaller than the effective threshold for this s_0, which can be estimated from Figure 14 to be around $\varepsilon = 0.69$.

of the jet velocity as the observable quantifying the amplitude of the perturbation is largely arbitrary. From our discussion of the relevance of perturbations, one might argue that s^*, on the other hand, provides a "meaningful" way of estimating the amplitude. Plotting the critical amplitude curve in terms of s^* instead of A can, *a priori*, completely change the nature of the extrapolated divergence. One can even imagine that s^* does not go to infinity when A does, in which case no divergence would be observed near R_c. Unfortunately, our experiments do not allow us to establish the precise mapping of s^* as a function of A, and we cannot, therefore, exclude this possibility.

6 Summary and perspectives

The parallel investigation — experimental and numerical — presented in this work has shown that the transition to turbulence in plane Couette flow is best interpreted, at a statistical level, as a discontinuous (first-order-like) transition to spatiotemporal intermittency.

We have stressed that only statistical arguments are valid in an experimental context, due to the unavoidably limited accuracy of initial conditions, the somewhat "blind" character of the way of introducing localized perturbations into the laminar flow, and the sensitivity to initial conditions expected whenever a chaotic attractor is involved. We have argued that the transition is only defined statistically even though the system is deterministic, and our results are indeed fully consistent with a threshold defined in terms of an equivalent probabilistic process. The threshold R_c can be seen as the value separating the regimes where the chaotic evolution among the unstable non-laminar solutions existing in phase space — such as the streamwise vortices [11]— can or cannot be sustained forever in time. No major structural change occurs in phase space at R_c. Extending this phase space picture a bit further, the Reynolds number R_u, below which all perturbations seem to decay quasi-monotonously (see Fig.6a), could be related, on the other hand, to the limit of existence of some of the nonlinear unstable solutions mentioned above. As a matter of fact, in spatially-extended systems showing spatiotemporal intermittency, the above-mentioned nonlinear objects cease to exist *below* the threshold. In the complex Ginzburg-Landau equation, for example, spatiotemporal intermittency regimes are easily observed. They involve localized objects (*e.g.* amplitude "holes") which exist, be they stable or unstable, in a region of parameter space that includes the border of existence of sustained spatiotemporal intermittency [28]. In plane Couette flow, the domain of existence of the solutions found recently seems to extend well-below $R = 325$ [5].

Our analysis has also pointed to the respective merits of quench and bubble experiments. Quench experiments may be sensitive to finite-size effects, but they allow one to explore directly the "natural" attractor or weak repellor of the system in phase space. Bubble experiments, and, more generally, all experiments in which localized perturbations are introduced externally, suffer from a certain degree of arbitrariness, if only because the structure of the phase space of the system is usually unknown. Our results have led to a proper definition of a "critical amplitude curve", and we have argued that this curve has no absolute significance. It depends on the type of localized perturbations performed, on the observable chosen to quantify their amplitude, and on the p-value chosen to determine the threshold. Even though a limited portion of one of these curves could be experimentally explored, the data suggests a divergence at R_c.

The general framework of the transition to spatiotemporal intermittency points to "universal" properties,

i.e. features expected to be independent of the details of the system. In the case of interest here, that of a discontinuous transition, one might wonder in particular whether the simple functional forms found experimentally and numerically for the divergence of the mean lifetime $\langle\tau\rangle$ in quench experiments below threshold are related. Our experimental results are consistent with $\langle\tau\rangle \sim (R_c - R)^{-1}$, while the numerical results yield $\langle\tau\rangle \sim (\varepsilon_c - \varepsilon)^{-2}$. We are not able to provide a rigorous argument linking these two simple numbers, but we believe the two exponents might indeed be related by a factor of two. We note, however, that a similar discussion comparing the nature of the divergence of the "critical amplitude" curves obtained does not make much sense in view of the relative arbitrariness of these curves and of the very limited portions explored in our experiments.

Our conclusions hold mostly at a qualitative level, and no detailed quantitative agreement is expected from the comparison of a phenomenon as complex as the intermittent turbulence present in plane Couette flow with a deliberately minimal coupled map lattice model. Should one want to construct a better model —we stress that this is not the intention of the present work—, one would have, at the very least, to change the coupling between sites to account for advection modes, and for possible long-range effects such as those suggested in [29] in the context of the spiral turbulence regime of Taylor-Couette flow.

Many of the questions above call for an experimental setup which would allow a more detailed investigation of the threshold region. The most crucial factor in this context is to increase the system size, and we hope that, in the future, carefully controlled experiments with, say, aspect ratios four times larger, will be performed. Next on the list of necessary modifications toward this aim is to change the way of creating localized perturbations to be able to explore a larger amplitude domain.

Finally, we wish that similar studies will be undertaken in the future to approach other outstanding problems in hydrodynamics such as plane Poiseuille flow.

We thank O. Dauchot, F. Daviaud and P. Manneville, for interesting discussions, and C. Gasquet and D. Popot for technical assistance in the acquisition and treatment of experimental data.

References

1. V.A. Romanov, Funkt. An. Prol. **7**, 137 (1970).
2. A. Lundbladh, A.V. Johansson, J. Fluid Mech. **229**, 499 (1991).
3. F. Daviaud, J. Hegseth, P. Bergé, Phys. Rev. Lett. **69**, 2511 (1992).
4. N. Tillmark, P.H. Alfredsson, J. Fluid Mech. **235**, 89 (1992).
5. M. Nagata, J. Fluid Mech. **217**, 519 (1990); R.M. Clever, F.H. Busse, J. Fluid Mech. **234**, 511 (1992).
6. A. Cherhabili, U. Ehrenstein, Eur. J. Mech. B / Fluids **14**, 677 (1995).
7. L.N. Trefethen, A.E. Trefethen, S.C. Reddy, T.A. Driscoll, Science **261**, 578 (1993); F. Waleffe, Studies in Appl. Math. **95**, 319 (1995).
8. For a general introduction to spatiotemporal intermittency, see, *e.g.*: H. Chaté, P. Manneville, in *Turbulence: A Tentative Dictionary*, edited by O. Cardoso, P. Tabeling (Plenum, New York, 1995).
9. W. Kinzel, in *Percolation Structures and Processes*, edited by G. Deutscher *et al.*, Ann. Israel Phys. Soc. **5**, 425 (1983).
10. S. Bottin, F. Daviaud, P. Manneville, O. Dauchot, Europhys. Lett. 1998, in press.
11. O. Dauchot, F. Daviaud, Phys. Fluids **7**, 901 (1995); N. Tillmark, Europhys. Lett. **32**, 481 (1995); S. Bottin, O. Dauchot, F. Daviaud, P. Manneville, preprint submitted to Phys. Fluids (1997).
12. This is the reason why plane Couette flow spontaneously transits to a turbulent regime at Reynolds numbers which vary with the experimental conditions. At a theoretical level, the decrease of metastability at large R has been considered by B. Dubrulle, S. Nazarenko, Europhys. Lett. **27**, 129 (1994).
13. O. Dauchot, P. Manneville, J. Phys. II France **7**, 371 (1997).
14. L.S. Schulman, P.E. Seiden, J. Stat. Phys. **19**, 293 (1978); R. Bidaux, N. Boccara, H. Chaté, Phys. Rev. A **39**, 3094 (1989).
15. Y. Pomeau, Physica D **23**, 3 (1986).
16. H. Chaté, in *Spontaneous Formation of Space-Time Structures and Criticality*, edited by T. Riste (Kluwer, Dordrecht, 1991).
17. H. Chaté, P. Manneville, Physica D **32**, 409 (1988); Physica D **37**, 33 (1989).
18. H. Chaté, P. Manneville, Europhys. Lett. **6**, 591 (1988).
19. Strictly speaking, the system size must be large enough for the exponentially small probability of decay always present in a finite system to be in practice negligible.
20. This requires the summability of the distribution, which is not insured *a priori*. However, this is the case of all examples studied in this work.
21. In the numerical experiments reported here, this effect is quite small.
22. O. Dauchot, F. Daviaud, Phys. Fluids **2**, 335 (1995).
23. J.C. Saut, R. Temam, *Attractor, inertial manifolds and their approximation, Conférence sur les systèmes dissipatifs en dimension infinie, Marseille.* Modélisation mathématique et analyse numérique, **83**, (1989).
24. This may explain the so-called "self-similar" structure found in [25] when plotting τ *vs.* R in numerical simulations modeling similar experiments. In view of our discussion, this may just be the consequence of $\tau(R)$ not being a function but rather a distribution which reflects the intrinsic sensitivity of the system to initial conditions.
25. A. Schmiegel, B. Eckhardt, Phys. Rev. Lett. **79**, 5250, (1997).
26. A.G. Darbyshire, T. Mullin, J. Fluid Mech. **289**, 83 (1995).
27. O. Dauchot, Ph.D. thesis, Université P.&M. Curie, Paris, 1995.
28. See, *e.g.* H. Chaté, Nonlinearity **7**, 185 (1994); M. van Hecke, Phys. Rev. Lett. **80**, 1896 (1998).
29. J.J. Hegseth, C.D. Andereck, F. Hayot, Y. Pomeau, Phys. Rev. Lett. **62**, 257 (1989); F. Hayot, Y. Pomeau, Phys. Rev. E **50**, 2019 (1994).